BIOCHEMISTRY
including biophysical chemistry & molecular biology

Article

pubs.acs.org/biochemistry

Conformationally Distinct Five-Coordinate Heme–NO Complexes of Soluble Guanylate Cyclase Elucidated by Multifrequency Electron Paramagnetic Resonance (EPR)

Alexander Gunn,[‡] Emily R. Derbyshire,[§] Michael A. Marletta,[§] and R. David Britt*[,‡]

[‡]Department of Chemistry, University of California, Davis, One Shields Avenue, Davis, California 95616, United States

[§]Departments of Molecular and Cellular Biology, QB3 Institute, and Division of Physical Biosciences, Lawrence Berkeley National Laboratory, University of California, Berkeley, California 94720-3220, United States

ABSTRACT: Soluble guanylate cyclase (sGC) is a heme-containing enzyme that senses nitric oxide (NO). Formation of a heme Fe–NO complex is essential to sGC activation, and several spectroscopic techniques, including electron paramagnetic resonance (EPR) spectroscopy, have been aimed at elucidating the active enzyme conformation. Of these, only EPR spectra (X-band ~9.6 GHz) have shown differences between low- and high-activity Fe–NO states, and these states are modeled in two different heme domain truncations of sGC, β1(1–194) and β2(1–217), respectively (Derbyshire et al., *Biochemistry* 2008, *47*, 3892–3899). The EPR signal of the low-activity sGC Fe–NO complex exhibits a broad lineshape that has been interpreted as resulting from site-to-site inhomogeneity, and simulated using *g* strain, a continuous distribution about the principal values of a given *g* tensor. This approach, however, fails to account for visible features in the X-band EPR spectra as well as the *g* anisotropy observed at higher microwave frequencies. Herein we analyze X-, Q-, and D-band EPR spectra and show that both the broad lineshape and the spectral structure of the sGC EPR signal at multiple microwave frequencies can be simulated successfully with a superposition of only two distinct *g* tensors. These tensors represent different populations that likely differ in Fe–NO bond angle, hydrogen bonding, or the geometry of the amino acid residues. One of these conformations can be linked to a form of the enzyme with higher activity.

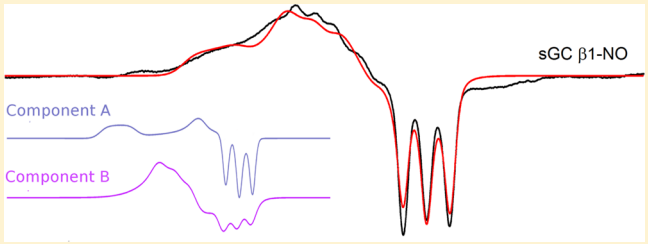

Soluble guanylate cyclase (sGC) catalyzes the formation of cyclic guanylate monophosphate (cGMP) from guanylate triphosphate (GTP). The synthesized cGMP is a secondary messenger for, and a critical step in, neuronal signaling, platelet aggregation, and vasodilation in mammals.[1−6] Binding of the radical diatomic gas nitric oxide (NO) to the heme cofactor is a key determinant of enzyme activation. sGC is a heterodimer that exists primarily of α1β1 subunits.[7] The β-subunit contains a heme-nitric oxide/oxygen binding (H–NOX) domain at the N-terminus, and a catalytic domain at the C-terminus. The α-subunit also contains a C-terminal catalytic domain, but does not bind heme. The heme cofactor in the β subunit is ligated by histidine, like in most globins, but it does not bind oxygen, and is stable in the ferrous-heme state. Upon NO binding, a six-coordinate intermediate conformation forms until the Fe–His bond breaks, producing a five-coordinate Fe^{II}–NO complex.[8−13]

The α1β1 sGC five-coordinate NO complex is known to exhibit low-activity in the presence of stoichiometric NO and GTP, and high-activity in the presence of the small molecule activator YC-1 or excess NO and GTP.[14,15] In addition to the ubiquitously expressed α1 and β1 subunits, a β2 subunit exists which is expressed largely in the kidney. N-terminal truncations of both β1 and β2 have been prepared and shown to bind heme and NO.[16]

The NO-bound form of full-length sGC and the β1 and β2 H–NOXs have been spectroscopically characterized. In electronic and vibrational spectroscopic studies, the truncated β1 and β2 H–NOX domains are reported as nearly indistinguishable.[16] In electron paramagnetic resonance (EPR) spectroscopy, however, the NO-heme EPR spectrum of the truncated β1 subunit strongly resembles that of the low-activity full-length protein, while the β2 truncation has an EPR spectrum that is similar to the spectrum of the high-activity sGC–NO state. This highly active form is characterized by a simple rhombic *g* tensor with *g* values listed in Table 1.

The inhomogeneous broadening of the spectral lines in sGC EPR spectra can be simulated using *g* strain, a model that assumes a Gaussian distribution of variations about each principal value. The *g* strain applied to sGC EPR spectra is anisotropic with a large *g* strain typically applied to the two higher *g* values, g_1 and g_2, and a smaller *g* strain is used on g_3, where the hyperfine splittings due to coupling to the nitrogen nucleus on the NO are more distinct.[17,18] EPR parameters determined by simulations using this strain model are given in Table 2. This model is effective for approximating the general lineshape of the X-band CW EPR spectra, as seen in Figure 1,

Received: June 20, 2012
Revised: September 14, 2012
Published: September 17, 2012

   dx.doi.org/10.1021/bi300831m | *Biochemistry* 2012, 51, 8384–8390

Table 1. Simulation Parameters for β2(1−217) sGC[a]

Sim model	parameter	1	2	3
X-band[b]	g	2.106	2.025	2.010
	g strain	0.0088	0.0090	0.0035
	A[d]	42.00	54.00	48.00
MF EPR[c]	g	2.1057	2.0245	2.0102
	g strain	0.0126	0.0093	0.0026
	A	42.73	55.35	47.71

[a]Values of the g and hyperfine tensors determined by X-band CW EPR only, reported previously,[18] and those determined in the present study by simultaneous fitting of X-, Q-, and D-band spectra (MF EPR). [b]Derbyshire et al. [c]This work. [d]Hyperfine coupling values in MHz are for ^{14}NO complexes.

Table 2. Simulation Parameters for β1(1−194) and β1(1−385) sGC Strain Model[a]

parameter	1	2	3
g	2.083	2.036	2.012
g strain	0.0345	0.0341	0.0047
A[b]	67.0	43.0	45.0

[a]These parameters are based on simulations of X-band spectra reported previously.[17,18] [b]Hyperfine coupling values in MHz are for ^{14}NO complexes.

but fails to account for some clear and reproducible spectral features in the g_1 and g_2 regions.

The EPR spectra of sGC and sGC H−NOX domains can be compared with spectra reported for other proteins with NO bound to a heme in a five-coordinate configuration, such as myoglobin and hemoglobin at low pH,[19−21] a bacterial H−NOX,[22] cysteine dioxygenase,[23] as well as nitrosyl-heme model compounds.[12,24−26] The continuous-wave (CW) EPR spectrum of five-coordinate ferrous-nitrosyl heme complexes at X-band, such as sGC, is characterized by a broad feature with $g_{max} \approx 2.07$, and a sharper triplet centered at $g = 2.01$.[10,17] Six-coordinate heme−NO EPR spectra typically have more hyperfine structure due to coupling to the histidine ligand. The hyperfine resolution is not as well-defined as in the five-coordinate case, however, so the overall effect is a general broadening.

Instead of a simulation model with a single g tensor with g strain, in this work we simulate the EPR spectrum of five-coordinate, NO-bound sGC using a two-component model. Herein, we show that this approach results in consistent fits for all the spectra measured over a broad frequency range (9−130 GHz).

MATERIALS AND METHODS

Sample Preparation. Samples of ^{14}NO and ^{15}NO complexes of rat sGC heme domain truncations β1(1−194), β1(1−385), and β2(1−217) were prepared for X-band CW EPR measurements according to a previously published procedure.[18] Protein concentrations for Q- and D-band samples ranged from 200 to 500 mM. NO gas was generated in all cases from acidified sodium nitrite ($Na^{14}NO_2$ or $Na^{15}NO_2$). Approximately 30 mL of the heme domain solutions were placed into Q-band quartz tubes, and at the same time, about 5 − 10 mL of each solution was placed into quartz capillaries for D-band measurements. Samples were stored at 77 K until spectra were collected. Quartz tubes for Q-Band EPR (1.10 mm ID, 1.60 mm OD) and D-Band capillaries (0.500 mm ID, 0.600 mm OD) were purchased from Vitrocom.

EPR Spectroscopy. EPR spectroscopy was performed at the University of California, Davis, CalEPR facility. CW X-band (9.66 GHz) EPR spectral data included in this report were previously published.[18] Q-band (35 GHz) and D-band (130 GHz) spectra were collected by electron spin echo (ESE) EPR, a pulsed EPR technique where a spin echo is generated from a Hahn sequence at each magnetic field, resulting in an absorption spectrum. The ESE EPR spectra were differentiated using a Savitsky-Golay 10-point smoothing with a numerical

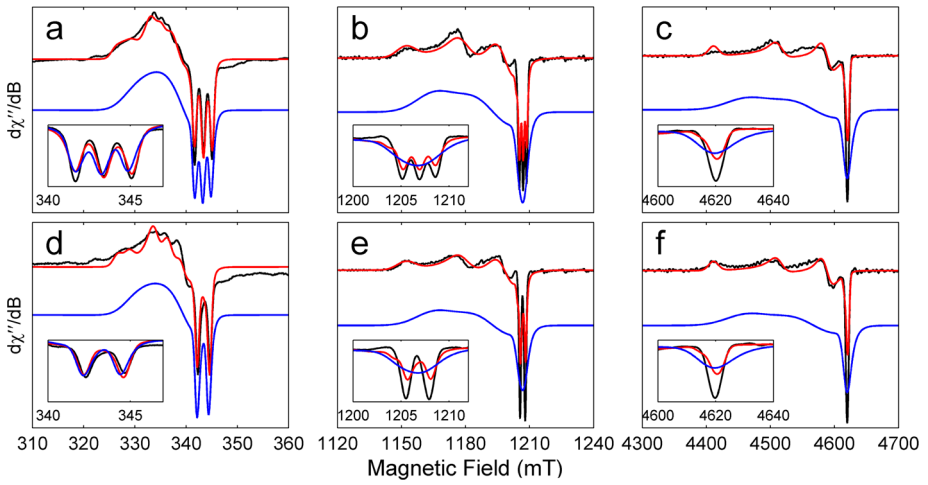

Figure 1. EPR spectra of β1 heme domain of sGC (black traces) are simulated at all frequencies using the two-component model (red trace), and the strain model (blue trace, offset below) reported previously. Q- and D-band data (b and e, and d and f) are the field derivatives of the absorption spectra obtained by ESE EPR. Simulation parameters are given in Table 1. Panels a, b, and c are the natural abundance ^{14}N spectra, and d, e, and f are spectra obtained with ^{15}N-labeled NO, the hyperfine couplings for the isotope labeling have been scaled by the ratio of the nuclear g values (eq 2). Insets show a close-up of the g_3 region of each spectrum with the corresponding simulations. X- and Q-band spectra were obtained at 25 K. X-band frequency was 9.66 GHz at 5.09 mW, 100 kHz modulation at 10.1 G with a time constant of 81.92 ms. Each spectrum is the average of 16 scans. Q-band frequency was 33.95 GHz at 4.823 mW with a $\pi/2$ pulse length of 20 ns and a τ of 230 ns, averaging 1000 echoes at a rep. time of 510 ms. D-band frequency was 129.996 GHz. Temperature was 10 K, $\pi/2$ pulse length was 50 ns and τ was 250 ns. 1300 echoes for ^{14}N samples, 1200 echoes for ^{15}N samples were acquired at a rep. time of 10 ms each.

dx.doi.org/10.1021/bi300831m | Biochemistry 2012, 51, 8384−8390

Table 3. EPR Parameters for Two-Component Model of β1 sGC Determined by Fitting Simulations to Multifrequency EPR Spectra[a]

	SysA			SysB			w_A/w_B
g	2.1057	2.0245	2.0102	2.0600	2.0580	2.0125	
A^{14}N	45.00	55.00	48.50	44.00	57.00	50.00	
A^{15}N	63.38	77.47	68.31	61.97	80.28	70.42	
H strain (X)	62.1992	61.4763	21.8738	252.3500	53.1058	35.2369	0.9635
H strain (Q)	283.8894	227.4899	25.0000	1002.8930	226.6543	25.0000	1.478
H strain (D)	518.8457	506.9550	100.0000	2517.1170	528.2815	100.0000	1.800

[a]Hyperfine and H strain values are in MHz.

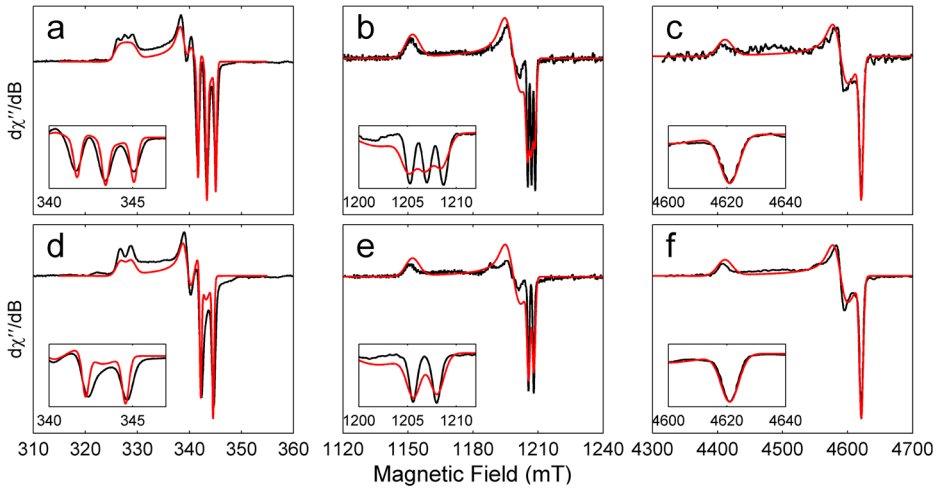

Figure 2. EPR spectra and simulations of β2 heme domain of sGC. The heme-domain EPR spectrum is shown in black, with the simulated spectrum in red. (a, b, c) β2(1−217)−^{14}NO. (d, e, f) β2(1−217)−^{15}NO. (a, d) X-band CW EPR. (b, e) Q-band ESE EPR differentiated by a 10-point Savitzky−Golay smoothing function. (c, f) D-band ESE EPR differentiated by the same method as were the Q-band spectra. Parameters for these multifrequency simulations are given in Table 1. The same parameters are used for all three frequencies. The hyperfine coupling values for the ^{15}N spectra are scaled by the ratio of nuclear g values (eq 2). Insets show a close-up of the g_3 region of each spectrum with the corresponding simulations. X- and Q-band spectra were obtained at 25 K. X-band frequency was 9.66 GHz at 5.09 mW, 100 kHz modulation at 10.1 G with a time constant of 81.92 ms. Each spectrum is the average of 16 scans. Q-band frequency was 33.95 GHz at 4.823 mW with a $\pi/2$ pulse length of 20 ns and a τ of 230 ns, averaging 1000 echoes at a rep. time of 510 ms. D-band frequency was 129.996 GHz. Temperature was 10 K, $\pi/2$ pulse length was 50 ns and τ was 250 ns. 1300 echoes for ^{14}N samples, 1200 echoes for ^{15}N samples were acquired at a rep. time of 10 ms each.

derivative to facilitate comparison of the echo-detected spectra with the CW spectra obtained previously.

X-band CW EPR spectra. X-band spectra were obtained using a Bruker ECS106 spectrometer, equipped with an Oxford Instruments ESR-900 helium flow cryostat. Experimental conditions were as follows: temperature, 25 K unless otherwise specified; microwave frequency, 9.66 GHz; microwave power, 5.09 mW; modulation frequency, 100 kHz; modulation amplitude, 10.1 G; and time constant, 81.92 ms. Each spectrum is the signal average of 16 scans. Q-band (35 GHz) absorption spectra were obtained on a Bruker E-580 ELEXSYS spectrometer. Absorption spectra were measured as the electron spin echo (ESE) intensity as a function of the applied magnetic field. Each spectrum was collected at 25 K and 4.823 mW with a $\pi/2$ pulse length of 20 ns and a τ of 230 ns. Each data point is the average of 1000 echoes at a rep. time of 510 ms. D-band (130 GHz) EPR absorption spectra were collected on a laboratory-constructed spectrometer operating at 129.996 GHz described previously.[27] The Field was varied with an 8-T cryogen-free superconducting magnet (Cryogenic Ltd., London). Temperature was 10 K, power was ∼100 mW with $\pi/2$ pulse equal to 50 ns and a τ of 250 ns and rep. time of 10 ms, 1300 echoes for ^{14}N samples, 1200 echoes for ^{15}N samples.

The magnetic field axis of the X-band data was calibrated using the spectrum of α,γ-bisdiphenylene-β-phenylallyl (BDPA). The field axis for Q-band spectra was calibrated with an NMR Tesla meter. For D-band measurements the external magnetic field was calibrated by comparison to equivalent spectra obtained by measuring the same sample with an added external standard, Mn(II) impurity in MgO.

Simulations of EPR Spectra. Simulations of EPR spectra were performed using EasySpin.[28] The g and hyperfine axes were assumed to be collinear for all systems in this report. The overall simulation, $F_{overall}$, is a linear combination of the two component simulations, F_A and F_B as shown in eq 1. The ratios for the scalars w_A and w_B are given in Table 3. The value of w_A with respect to w_B represent the best fit to the data. The physical significance of the relative increase in component A at the higher frequencies is unclear. The samples were kept frozen in liquid nitrogen, therefore conformational changes at each field are unlikely, and the deviations from unity may simply reflect approximations in the model.

$$F_{overall} = w_A{*}F_A + w_B{*}F_B \quad (1)$$

Values for g tensors in multifrequency EPR simulations were determined from the field positions of spectral features in the D-band EPR spectra. At this frequency, the hyperfine structure

dx.doi.org/10.1021/bi300831m | Biochemistry 2012, 51, 8384−8390

is obscured by the inhomogeneously broadened lineshape, so the spectrum is almost completely determined by the g anisotropy. Hyperfine coupling values were determined from a least-squares fit of the X-band spectra. Linewidths were then determined by a genetic algorithm fit to data at each of the three frequencies measured. The g axis and hyperfine axis were assumed to be collinear for all systems in this report. Hyperfine coupling values for isotope substitution experiments were scaled by the ratio of the nuclear g values according to eq 2 so that ^{14}N and ^{15}N spectra could be fit simultaneously.

$$A^{14}{}_{N} = A^{15}{}_{N}(g^{14}{}_{N}/g^{15}{}_{N}) = A^{15}{}_{N}*0.71 \quad (2)$$

Line broadening was fit at each microwave frequency. This allowed the lineshape to be treated independent of possible differences in sample freezing or other variables that could have a potential effect on the overall lineshape, leaving the focus on the g tensor and hyperfine couplings as the common parameters among all spectra. Broadening in $\beta1$ simulations was modeled as H strain only, and in $\beta2$ simulations as g strain only.

RESULTS AND DISCUSSION

Figures 1 and 2 show the spectra obtained by EPR at multiple frequencies. The higher-field spectra in Figure 1 clearly show an increased resolution of the g values, and inadequacy of the strain model in simulating these spectra. The two-component simulations succeed in fitting the spectral features at all frequencies while the approximation of the spectral lineshape given by the strain model quickly falls apart at Q- and D-band. The $\beta2$ spectra, however, continue to be fit satisfactorily by those parameters (Table 1) determined by the X-band data alone, even up to 130 GHz.

The simulation model used in Derbyshire et al.[18] for the X-band spectrum of $\beta2$ H−NOX employed a single spectral component. Selecting a minimal number of conformations, rather than the continuum modeled by g strain, both $\beta1$(1−194) and full-length sGC EPR spectra can be satisfactorily simulated as the sum of two different signals. The g and A tensors used to simulate $\beta2$ H−NOX are similar to component A of the $\beta1$ H−NOX simulations (Table 3), suggesting the $\beta1$ H−NOX may be a mixture that contains a population of protein with a conformation similar to that of the $\beta2$ H−NOX.

Kinetic data for the dissociation of NO for both the $\beta1$ and $\beta2$ H-NOX constructs of sGC, as well as the full-length protein, have been modeled as an equilibrium of two conformations, each with a different dissociation rate.[29] From this data, the sGC-NO complex was interpreted to exist as a mixture of two five-coordinate states. Despite the observation, however, that both $\beta1$ and $\beta2$ H-NOX domains showed similar two-component kinetic behavior, the more-active and less-active conformations that correspond to the two EPR spectral components A and B are different for the $\beta1$ and $\beta2$ cases. That is, though the same two conformations that determine the NO dissociation mechanism exist in both truncations, in the current EPR analysis only the conformation that corresponds to the spectral component A is contributing to the EPR spectrum of the $\beta2$ H-NOX. Therefore, it is likely that the two sGC conformations of different enzyme activity that are observed by EPR are not the same conformations that give rise to the observed fast and slow NO dissociation kinetics.

Differences in the EPR signal of sGC under 1 equiv of NO and excess NO have been noted.[18] Hyperfine structure is visible in the spectrum under excess NO that is obscured when only a stoichiometric amount of NO is added to the enzyme. The additional structure has an appearance that resembles the spectrum of the $\beta2$ H−NOX complex, but still has some of the broad features that are not present in the $\beta2$ spectrum. Under the two-component model this change in the spectral shape of the EPR signal suggests that a second NO can bind to the sGC−NO complex in a way that results in a conformation consistent with an increase in the population of the Fe^{II}−NO species characterized by signal A. A report on NO binding kinetics to sGC under excess NO observed the EPR spectrum of six-coordinate sGC conformation and of stable five-coordinate conformations.[8] The additional hyperfine structure expected from coupling to the His nitrogen is visible in the six-coordinate transient spectrum. The g values of this intermediate, reported as 2.097, 2.018, and 1.985, are similar to, though shifted upfield from the values reported for the rhombic component A in the current two-component analysis. The five-coordinate spectrum is assigned by Martin and co-workers as an axial powder pattern with $g_x = g_y = 2.076$ and $g_z = 2.008$ (see Table 4). The activity of sGC is known to increase with excess NO, compared to the case where a stoichiometric amount of NO is added, which is consistent with the interpretation that spectral component A represents a highly active state.

Table 4. g Tensor Values Used to Simulate EPR Spectra of sGC and Other Nitrosyl Heme Complexes According to the Linear Combination of Spectral Simulations Described in eq 1

protein	signal	g_1	g_2	g_3
sGC $\beta1^a$	A	2.1057	2.0245	2.0102
sGC $\beta1^a$	B	2.0600	2.0580	2.0125
sGC $\beta2^a$		2.1057	2.0245	2.0102
sGC^b		2.0830	2.0360	2.0120
6c-sGC^c		2.097	2.018	1.985
5c-sGC^d			2.076	2.008
Mb^e	A	2.080	1.979	1.998
Mb^e	B		2.041	1.98
Mb^f	A	2.075	2.008	1.987
Mb^f	B		2.030	1.98
WT NIR^g	A	2.062	2.004	1.960
WT NIR^g	B	2.076	2.025	1.953

^{a}Two-component simulations from this work. ^{b}Strain model used for sGC in Derbyshire et al.[18] ^{c}Six-coord sGC intermediate from Martin et al.[8] ^{d}Five-coord sGC from Martin et al.[8] ^{e}Six-coord myoglobin from Morse and Chan.[32] ^{f}Six coord myoglobin from Radoul et al.[30] ^{g}Six-coord nitrite reductase from Radoul et al.[31]

The allosteric activators YC-1 and BAY 41−2272 have been modeled with a single g tensor, and spectral differences relative to native sGC were described as linewidth narrowing accompanied by a shift in g values.[18] In the current analysis the spectrum of the activated sGC can be interpreted, instead, as arising from a conformation consistent with spectral component A.

The anisotropy in the spectrum for a given g tensor becomes more pronounced with increasing magnetic field, while the hyperfine is largely independent of the magnetic field. The resulting effect is that the higher-frequency, or higher-field, spectra display fewer spectral features than the lower-frequency spectra because the spectral linewidth at a given field position

dx.doi.org/10.1021/bi300831m | Biochemistry 2012, 51, 8384−8390

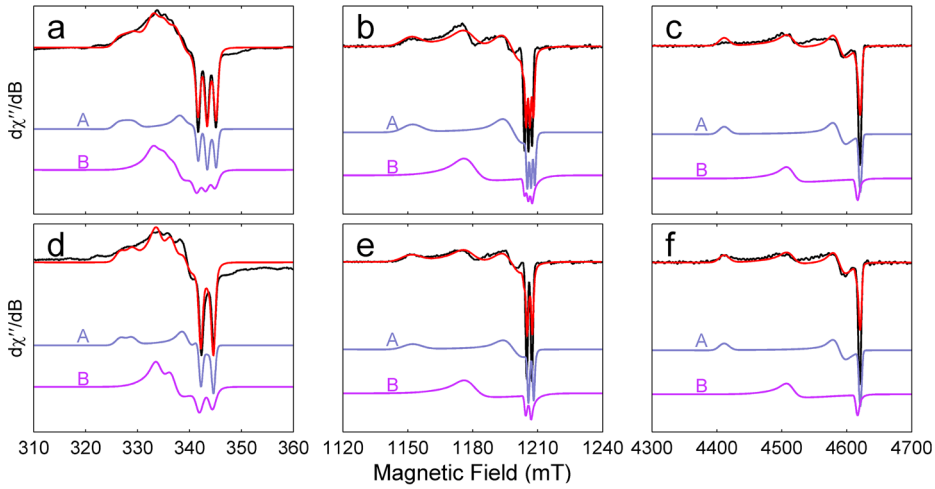

Figure 3. Simulations of the β1 heme domain data with components A and B. The simulation of each contributing g tensor is shown, offset, along with the weighted sum (red trace), and the spectral data (black trace) as in Figure 1. Simulations of component A are offset below the data, with those of component B offset further below that. The relative fraction of A to B used in the X-, Q-, and D-band spectra is 0.9635, 1.478, and 1.800, respectively. X- and Q-band spectra were obtained at 25 K. X-band frequency was 9.66 GHz at 5.09 mW, 100 kHz modulation at 10.1 G with a time constant of 81.92 ms. Each spectrum is the average of 16 scans. Q-band frequency was 33.95 GHz at 4.823 mW with a $\pi/2$ pulse length of 20 ns and a τ of 230 ns, averaging 1000 echoes at a rep. time of 510 ms. D-band frequency was 129.996 GHz. Temperature was 10 K, $\pi/2$ pulse length was 50 ns and τ was 250 ns. 1300 echoes for ^{14}N samples, 1200 echoes for ^{15}N samples were acquired at a rep. time of 10 ms each.

may be significantly greater than the hyperfine splittings. This distinction between spectral features arising from g anisotropy and features that are split by the hyperfine interaction at different microwave frequencies allows the determination of appropriate spin Hamiltonian terms by measurement of the sample at several EPR frequencies. The disagreement between the g anisotropy of the previously published strain distribution model[17,18] and that of the observed spectra shown in Figure 1 becomes very pronounced at Q- and D-band, where the hyperfine structure observed at lower frequencies is overshadowed in the overall lineshape.

Linewidth changes and relative field positions observed at different microwave frequencies are consistent with the spread of g values in the simulation, especially the spectral turning points for each component that are more visible at higher fields. If the broadening were due only to a continuous distribution of overlapping g values spread by site-to-site inhomogeneity, that is, if the linewidth were to be attributed to g strain only, then the turning points indicating the larger g values would be as obscured in the Q- and D-band spectra as they are at X-band. Such is the case represented by the strain-model simulations shown in Figure 1 (lower trace in each frame). Additionally, the more resolved features of the X-band EPR spectrum visible at g_1 and g_2 cannot be reproduced by using a single g tensor simulation invoking g strain to fit the simulation to the overall width of the spectrum.

In Figure 3 the two-component simulations from Figure 1 are shown along with the individual component spectra. There is a significant difference in the lineshapes of components A and B. The former is characterized by a rhombic g tensor with principal values of g_1 = 2.1057, g_2 = 2.0245, and g_3 = 2.0102. Component B, on the other hand, has a nearly axial lineshape with $g_1 \approx g_2 \approx 2.06$, and g_3 = 2.0125. The overall lineshape of the simulated spectrum composed from the sum[1] fits the experimental spectrum consistently at all frequencies.

Recently the W-band EPR spectrum of the myoglobin six-coordinate Fe−NO complex was simulated as a superposition of a rhombic powder pattern and an axial powder pattern,[30] and a similar analysis was applied to nitrite reductase (NIR),[31] also a six-coordinate nitrosyl-heme protein. The g tensors used for these simulations are included in Table 4. This two-component analysis of the six-coordinate nitrosyl-heme EPR spectra is based on two spectral components identified in a temperature dependence study.[32] The relative contributions to the EPR spectrum from each component in these cases were seen to shift from a predominately rhombic spectrum to a more axial form as the temperature increased. The temperature dependence of the two-component EPR signals of sGC (Figure 4), however, does not display the same population shift from one conformation into the other. This observed behavior, added to the difference in g values between five- and six-coordinate complexes as shown in Table 4, suggests that the conformations and hydrogen bonding interactions of the NO ligand that are contributing to the EPR spectra are not the same for the six-coordinate case as for the five-coordinate case, and that the conformations of the Fe^{II}−NO species are essentially independent of temperature in the studied range. There is a possibility that the two conformations that give rise to the EPR spectra are two nearly degenerate orientations of the NO with respect to the heme plane. Further studies involving DFT calculations to determine the relative energies of this system more precisely could confirm this potential interpretation.

Scholes and colleagues[9] reported an X-band EPR spectrum for wild-type NO-bound cytochrome c′ (cytc′ −NO), a five-coordinate heme−NO protein, that is similar in appearance to the β2 H−NOX domain spectrum. The EPR spectrum of the R127A mutant of cytc′ −NO shows that the spectrum shifts to a signal that closely resembles that of the β1 H−NOX domain and that of full-length sGC. This drastic change in the g values of cytc′ −NO R127A suggests that there is a subtle, but significant change in the coordinate bonding in the different conformations and it is known that this spectroscopic change accompanies a change in the hydrogen bonding. This change likely corresponds to a heme−NO conformation that is equivalent to component A of the current sGC analysis. Thus the observed change in the EPR signal of sGC could be induced

dx.doi.org/10.1021/bi300831m | *Biochemistry* 2012, 51, 8384−8390

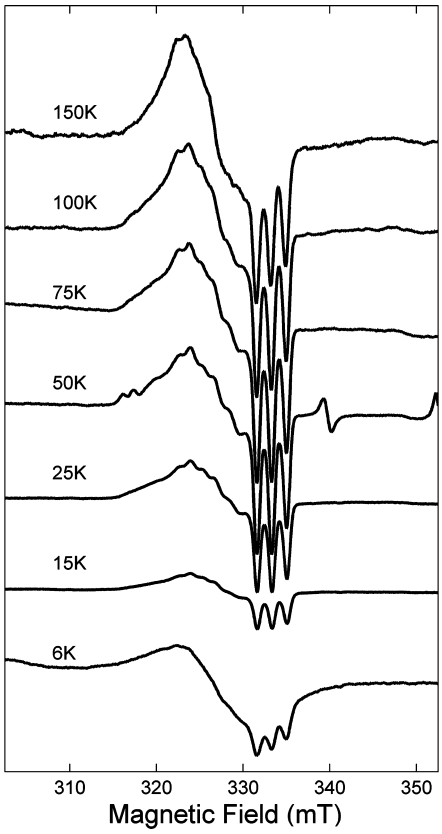

Figure 4. Temperature dependence of β1(1−385) sGC X-band CW EPR spectra. Subtle line shape changes accompany changes in temperature; however there is no distinct shift in the relative populations of the axial and rhombic g tensors, as was reported for six-coordinate nitrosyl hemes.[30,32] Each spectrum has been scaled by the absolute temperature at which the spectrum was measured.

by changes in the hydrogen-bonding partners of the bound NO. No obvious hydrogen-bond donor has been identified, however, in the distal heme pocket of sGC based on homology modeling. Therefore, a hydrogen-bond proton in sGC must come from either a water molecule or from the peptide backbone.

There is little variation of the smallest g value, g_3, among the five-coordinate sGC complexes simulated in this work. This is consistent with the single crystal nuclear resonance vibrational spectroscopy (NRVS) results from a nitrosyl heme model compound, and DFT predictions that show that g_3 is the g tensor component that is most parallel to the Fe−N bond, and is not significantly affected by the direction of the NO bond.[12] Meanwhile, the other two g values are predicted to vary when the NO ligand is in different orientations with respect to the porphyrin ring.[12] This provides an explanation of the shape of the five-coordinate EPR spectrum—the broad low-field feature is the superposition of multiple orientations of the NO ligand, and the well resolved hyperfine splittings at the higher-field g_3 portion of the spectrum persists with any number of orientations included.[2] A large number of such orientations is equivalent to the strain model shown in Figure 1. The two-component simulation model could correlate with two specific orientations of the NO ligand. These orientations would then represent the high- and low-activity states.

A study also showed that in the six-coordinate case none of the g tensor components are collinear with the Fe−NO bond axis.[2] Therefore, a well-resolved triplet would not be expected for a six-coordinate heme−NO complex according to the argument given above, as is indeed the case. The EPR spectra of five-coordinate model compounds clearly match the sGC spectra reported here, confirming other reports that sGC exists exclusively as a five-coordinate species.[33−35]

The g tensors of other nitrosyl heme systems are reported to depend on the hydrogen bonding environment around the nitrosyl oxygen. In particular, the broad features of five-coordinate heme−NO complexes have been interpreted as the sum of many NO orientations. The results of this report suggest that there may be two stable orientations with respect to the porphyrin ring. Considering the agreement of the two-component simulation model with the spectral features of β1 H−NOX at several EPR frequencies, it is likely that only two Fe^{II}−NO conformations are needed to interpret the structural and chemical properties five-coordinate nitrosyl heme systems.

■ CONCLUSIONS

Taken together, this work shows that the sGC−NO complex exists as a mixture of two spectroscopically distinct conformations. These conformations correlate with different activities, and the activation state of sGC can be determined simply by EPR spectroscopy. Multifrequency EPR analysis has enabled simulations of these two Fe^{II}−NO states and provided g values that can be related to the electronic structure of the component states. Additionally, the conformational change that shifts the Fe^{II}−NO complex from a low-activity to a high-activity state in the presence of YC-1 or excess NO and GTP, involves an increase in the abundance in component A of the β1 H−NOX spectrum. Therefore, the conformation that is observed in these activated complexes and in the β2(1−217)−NO complex is the conformation with the greatest catalytic activity. Shifts to this high-activity conformation may also have an important role in modulating sGC activity in the presence of excess NO or other conditions.

■ AUTHOR INFORMATION

Corresponding Author

*E-mail: rdbritt@ucdavis.edu. Tel: 530-752-6377.

Funding

This work was supported by grants from the National Institutes of Health, GM073789 (R.D.B.) and GM077365 (M.A.M.).

Notes

The authors declare no competing financial interest.

■ REFERENCES

(1) Derbyshire, E. R., and Marletta, M. A. (2009) Biochemistry of soluble guanylate cyclase. *Handb. Exp. Pharmacol. 191*, 17−31.

(2) Goodrich, L. E., Paulat, F., Praneeth, V. K. K., and Lehnert, N. (2010) Electronic Structure of Heme-Nitrosyls and Its Significance for Nitric Oxide Reactivity, Sensing, Transport, and Toxicity in Biological Systems. *Inorg. Chem. 49*, 6293−6316.

(3) Buechler, W. A., Ivanova, K., Wolfram, G., Drummer, C., Heim, J. M., and Gerzer, R. (1994) Platelet-Dependent Vascular Occlusion, in Annals of the New York Academy of Sciences (Fitzgerald, G. A., Jennings, L. K., Patrono, C., Eds.) Vol. *714*, pp 151−157, New York Academy of Sciences, New York.

(4) Denninger, J. W., and Marletta, M. A. (1999) Guanylate cyclase and the NO/cGMP signaling pathway. *BBA-Bioenergetics 1411*, 334−350.

(5) Munzel, T., Feil, R., Mulsch, A., Lohmann, S. M., Hofmann, F., and Walter, U. (2003) Physiology and pathophysiology of vascular

signaling controlled by cyclic guanosine 3′,5′-cyclic monophosphate-dependent protein kinase. *Circulation 108*, 2172−2183.
(6) Warner, T. D., Mitchell, J. A., Sheng, H., and Murad, F. (1994) Effects of Cyclic [GMP] on Smooth Muscle Relaxation, in *Adv. Pharmacol.* (Murad, F., Ed.) Vol. *26*; pp 171−194, Academic Press, New York.
(7) Kamisaki, Y., Saheki, S., Nakane, M., Palmieri, J. A., Kuno, T., Chang, B. Y., Waldman, S. A., and Murad, F. (1986) Soluble guanylate cyclase from rat lung exists as a heterodimer. *J. Biol. Chem. 261*, 7236−7241.
(8) Martin, E., Berka, V., Sharina, I., and Tsai, A.-L. (2012) Mechanism of Binding of NO to Soluble Guanylyl Cyclase: Implication for the Second NO Binding to the Heme Proximal Site. *Biochemistry 51*, 2737−2746.
(9) Lee, B., Usov, O. M., Grigoryants, V. M., Myers, W. K., Shapleigh, J. P., and Scholes, C. P. (2009) The Role of Arginine-127 at the Proximal NO-Binding Site in Determining the Electronic Structure and Function of 5-Coordinate NO-Heme in Cytochrome c′ of Rhodobacter sphaeroides. *Biochemistry 48*, 8985−8993.
(10) Lehnert, N., Sage, J. T., Silvernail, N., Scheidt, W. R., Alp, E. E., Sturhahn, W., and Zhao, J. (2010) Oriented Single-Crystal Nuclear Resonance Vibrational Spectroscopy of [Fe(TPP)(MI)(NO)]: Quantitative Assessment of the trans Effect of NO. *Inorg. Chem. 49*, 7197−7215.
(11) Poulos, T. L. (2006) Soluble guanylate cyclase. *Curr. Opin. Struct. Biol. 16*, 736−743.
(12) Praneeth, V. K. K., Näther, C., Peters, G., and Lehnert, N. (2006) Spectroscopic Properties and Electronic Structures of Five- and Six-Coordinate Iron(II) Porphyrin NO Complexes: Effect of the Axial N-Donor Ligand. *Inorg. Chem. 45*, 2795−2811.
(13) Zhao, Y., Hoganson, C., Babcock, G. T., and Marletta, M. A. (1998) Structural Changes in the Heme Proximal Pocket Induced by Nitric Oxide Binding to Soluble Guanylate Cyclase. *Biochemistry 37*, 12458−12464.
(14) Cary, S. P. L., Winger, J. A., and Marletta, M. A. (2005) Tonic and acute nitric oxide signaling through soluble guanylate cyclase is mediated by nonheme nitric oxide, ATP, and GTP. *Proc. Natl. Acad. Sci. U.S.A. 102*, 13064−13069.
(15) Russwurm, M., and Koesling, D. (2004) NO activation of guanylyl cyclase. *EMBO J. 23*, 4443−4450.
(16) Karow, D. S., Pan, D., Davis, J. H., Behrends, S., Mathies, R. A., and Marletta, M. A. (2005) Characterization of Functional Heme Domains from Soluble Guanylate Cyclase. *Biochemistry 44*, 16266−16274.
(17) Stone, J. R., Sands, R. H., Dunham, W. R., and Marletta, M. A. (1995) Electron Paramagnetic Resonance Spectral Evidence for the Formation of a Pentacoordinate Nitrosyl-Heme Complex on Soluble Guanylate Cyclase. *Biochem. Biophys. Res. Commun. 207*, 572−577.
(18) Derbyshire, E. R., Gunn, A., Ibrahim, M., Spiro, T. G., Britt, R. D., and Marletta, M. A. (2008) Characterization of two different five-coordinate soluble guanylate cyclase ferrous-nitrosyl complexes. *Biochemistry 47*, 3892−3899.
(19) Ascenzi, P., Giacometti, G. M., Antonini, E., Rotilio, G., and Brunori, M. (1981) Equilibrium and Kinetic Evidence for a Transition between Six- and Five-coordinate Ferrous Heme in the Nitric Oxide Derivative of Aplysia Myoglobin. *J. Biol. Chem. 256*, 5383−5386.
(20) Kon, H. (1968) Paramagnetic Resonance Study of Nitric Oxide Hemoglobin. *J. Biol. Chem. 243*, 4350−4357.
(21) Schmidt, P. P., Kappl, R., and Hüttermann, J. (2001) On the Mode of Hexacoordinated NO Binding to Myo- and Hemoglobin: Variable-Temperature EPR Studies at Multiple Microwave Frequencies. *Appl. Magn. Reson. 21*, 423−440.
(22) Tsai, A.-L., Berka, V., Martin, F., Ma, X., van den Akker, F., Fabian, M., and Olson, J. S. (2010) Is Nostoc H-NOX a NO sensor or Redox Switch? *Biochemistry 49*, 6587−6599.
(23) Pierce, B., Gardner, J. D., Bailey, L. J., Brunold, T. C., and Fox, B. G. (2007) Characterization of the Nitrosyl Adduct of Substrate-Bound Mouse Cysteine Dioxygenase by Electron Paramagnetic Resonance: Electronic Structure of the Active Site and Mechanistic Implications. *Biochemistry 46*, 8569−8578.
(24) Berto, T. C., Praneeth, V. K. K., Goodrich, L. E., and Lehnert, N. (2009) Iron-Porphyrin NO Complexes with Covalently Attached N-Donor Ligands: Formation of a Stable Six-Coordinate Species in Solution. *J. Am. Chem. Soc. 131*, 17116−17126.
(25) Paulat, F., Berto, T. C., George, S. D., Goodrich, L., Praneeth, V. K. K., Sulok, C. D., and Lehnert, N. (2008) Vibrational Assignments of Six-Coordinate Ferrous Heme Nitrosyls: New Insight from Nuclear Resonance Vibrational Spectroscopy. *Inorg. Chem. 47*, 11449−11451.
(26) Praneeth, V. K. K., Neese, F., and Lehnert, N. (2005) Spin Density Distribution in Five- and Six-Coordinate Iron(II)-Porphyrin NO Complexes Evidenced by Magnetic Circular Dichroism Spectroscopy. *Inorg. Chem. 44*, 2570−2572.
(27) Stich, T. A., Lahiri, S., Yeagle, G., Dicus, M., Brynda, M., Gunn, A., Aznar, C., DeRose, V. J., and Britt, R. D. (2007) Multifrequency pulsed EPR studies of biologically relevant manganese(II) complexes. *Appl. Magn. Reson. 31*, 321−341.
(28) Stoll, S., and Schweiger, A. (2006) EasySpin, a comprehensive software package for spectral simulation and analysis in EPR. *J. Magn. Reson. 178*, 42−55.
(29) Winger, J. A., Derbyshire, E., and Marletta, M. A. (2007) Dissociation of Nitric Oxide from Soluble Guanylate Cyclase and Heme-Nitric Oxide/Oxygen Binding Domain Constructs. *J. Biol. Chem. 282*, 897−907.
(30) Radoul, M., Sundararajan, M., Potapov, A., Riplinger, C., Neese, F., and Goldfarb, D. (2010) Revisiting the nitrosyl complex of myoglobin by high-field pulse EPR spectroscopy and quantum mechanical calculations. *Phys. Chem. Chem. Phys. 12*, 7276−7289.
(31) Radoul, M., Bykov, D., Rinaldo, S., Cutruzzolà, F., Neese, F., and Goldfarb, D. (2011) Dynamic Hydrogen-Bonding Network in the Distal Pocket of the Nitrosyl Complex of Pseudomonas aeruginosa cd1 Nitrite Reductase. *J. Am. Chem. Soc. 133*, 3043−3055.
(32) Morse, R. H., and Chan, S. I. (1980) Electron paramagnetic resonance studies of nitrosyl ferrous heme complexes. Determination of an equilibrium between two conformations. *J. Biol. Chem. 255*, 7876−7882.
(33) Kadish, K., Smith, K., Guilard, R. (1999) *The Porphyrin Handbook: Biochemistry and Binding: Activation of Small Molecules*, Vol. *4*, Academic Press, New York.
(34) Stone, J. R., and Marletta, M. A. (1994) Soluble Guanylate Cyclase from Bovine Lung: Activation with Nitric Oxide and Carbon Monoxide and Spectral Characterization of the Ferrous and Ferric States. *Biochemistry 33*, 5636−5640.
(35) Zhao, Y., Brandish, P. E., Ballou, D. P., and Marletta, M. A. (1999) A molecular basis for nitric oxide sensing by soluble guanylate cyclase. *Proc. Natl. Acad. Sci. U.S.A. 96*, 14753−14758.